

University of Nebraska - Lincoln

DigitalCommons@University of Nebraska - Lincoln

Kenneth Bloom Publications

Research Papers in Physics and Astronomy

5-4-1998

Observation of the Radiative Decay $D^{*+} \rightarrow D^+ \gamma$

J. Bartelt

Vanderbilt University, Nashville, Tennessee

Kenneth A. Bloom

University of Nebraska-Lincoln, kenbloom@unl.edu

CLEO Collaboration

Follow this and additional works at: <https://digitalcommons.unl.edu/physicsbloom>



Part of the [Physics Commons](#)

Bartelt, J.; Bloom, Kenneth A.; and Collaboration, CLEO, "Observation of the Radiative Decay $D^{*+} \rightarrow D^+ \gamma$ " (1998). *Kenneth Bloom Publications*. 150.

<https://digitalcommons.unl.edu/physicsbloom/150>

This Article is brought to you for free and open access by the Research Papers in Physics and Astronomy at DigitalCommons@University of Nebraska - Lincoln. It has been accepted for inclusion in Kenneth Bloom Publications by an authorized administrator of DigitalCommons@University of Nebraska - Lincoln.

Observation of the Radiative Decay $D^{*+} \rightarrow D^+ \gamma$

J. Bartelt,¹ S.E. Csorna,¹ V. Jain,^{1,*} K.W. McLean,¹ S. Marka,¹ R. Godang,² K. Kinoshita,² I.C. Lai,² P. Pomianowski,² S. Schrenk,²¹ G. Bonvicini,³ D. Cinabro,³ R. Greene,³ L.P. Perera,³ G.J. Zhou,³ B. Barish,⁴ M. Chadha,⁴ S. Chan,⁴ G. Eigen,⁴ J.S. Miller,⁴ C. O'Grady,⁴ M. Schmidtler,⁴ J. Urheim,⁴ A.J. Weinstein,⁴ F. Würthwein,⁴ D.W. Bliss,⁵ G. Masek,⁵ H.P. Paar,⁵ S. Prell,⁵ V. Sharma,⁵ D.M. Asner,⁶ J. Gronberg,⁶ T.S. Hill,⁶ D.J. Lange,⁶ R.J. Morrison,⁶ H.N. Nelson,⁶ T.K. Nelson,⁶ J.D. Richman,⁶ D. Roberts,⁶ A. Ryd,⁶ M.S. Witherell,⁶ R. Balest,⁷ B.H. Behrens,⁷ W.T. Ford,⁷ A. Gritsan,⁷ H. Park,⁷ J. Roy,⁷ J.G. Smith,⁷ J.P. Alexander,⁸ C. Bebek,⁸ B.E. Berger,⁸ K. Berkelman,⁸ K. Bloom,⁸ V. Boisvert,⁸ D.G. Cassel,⁸ H.A. Cho,⁸ D.S. Crowcroft,⁸ M. Dickson,⁸ S. von Dombrowski,⁸ P.S. Drell,⁸ K.M. Ecklund,⁸ R. Ehrlich,⁸ A.D. Foland,⁸ P. Gaidarev,⁸ L. Gibbons,⁸ B. Gittelman,⁸ S.W. Gray,⁸ D.L. Hartill,⁸ B.K. Heltsley,⁸ P.I. Hopman,⁸ J. Kandaswamy,⁸ P.C. Kim,⁸ D.L. Kreinick,⁸ T. Lee,⁸ Y. Liu,⁸ N.B. Mistry,⁸ C.R. Ng,⁸ E. Nordberg,⁸ M. Ogg,^{8,†} J.R. Patterson,⁸ D. Peterson,⁸ D. Riley,⁸ A. Soffer,⁸ B. Valant-Spaight,⁸ C. Ward,⁸ M. Athanas,⁹ P. Avery,⁹ C.D. Jones,⁹ M. Lohner,⁹ C. Prescott,⁹ J. Yelton,⁹ J. Zheng,⁹ G. Brandenburg,¹⁰ R.A. Briere,¹⁰ A. Ershov,¹⁰ Y.S. Gao,¹⁰ D.Y.-J. Kim,¹⁰ R. Wilson,¹⁰ H. Yamamoto,¹⁰ T.E. Browder,¹¹ Y. Li,¹¹ J.L. Rodriguez,¹¹ T. Bergfeld,¹² B.I. Eisenstein,¹² J. Ernst,¹² G.E. Gladding,¹² G.D. Gollin,¹² R.M. Hans,¹² E. Johnson,¹² I. Karliner,¹² M.A. Marsh,¹² M. Palmer,¹² M. Selen,¹² J.J. Thaler,¹² K.W. Edwards,¹³ A. Bellerive,¹⁴ R. Janicek,¹⁴ D.B. MacFarlane,¹⁴ P.M. Patel,¹⁴ A.J. Sadoff,¹⁵ R. Ammar,¹⁶ P. Baringer,¹⁶ A. Bean,¹⁶ D. Besson,¹⁶ D. Coppage,¹⁶ C. Darling,¹⁶ R. Davis,¹⁶ S. Kotov,¹⁶ I. Kravchenko,¹⁶ N. Kwak,¹⁶ L. Zhou,¹⁶ S. Anderson,¹⁷ Y. Kubota,¹⁷ S.J. Lee,¹⁷ J.J. O'Neill,¹⁷ S. Patton,¹⁷ R. Poling,¹⁷ T. Riehle,¹⁷ A. Smith,¹⁷ M.S. Alam,¹⁸ S.B. Athar,¹⁸ Z. Ling,¹⁸ A.H. Mahmood,¹⁸ H. Severini,¹⁸ S. Timm,¹⁸ F. Wappler,¹⁸ A. Anastassov,¹⁹ J.E. Duboscq,¹⁹ D. Fujino,^{19,‡} K.K. Gan,¹⁹ T. Hart,¹⁹ K. Honscheid,¹⁹ H. Kagan,¹⁹ R. Kass,¹⁹ J. Lee,¹⁹ M.B. Spencer,¹⁹ M. Sung,¹⁹ A. Undrus,^{19,§} R. Wanke,¹⁹ A. Wolf, M.M. Zoeller,¹⁹ B. Nemati,²⁰ S.J. Richichi,²⁰ W.R. Ross,²⁰ P. Skubic,²⁰ M. Bishai,²¹ J. Fast,²¹ J.W. Hinson,²¹ N. Menon,²¹ D.H. Miller,²¹ E.I. Shibata,²¹ I.P.J. Shipsey,²¹ M. Yurko,²¹ S. Glenn,²² S.D. Johnson,²² Y. Kwon,^{22,||} S. Roberts,²² E.H. Thorndike,²² C.P. Jessop,²³ K. Lingel,²³ H. Marsiske,²³ M.L. Perl,²³ V. Savinov,²³ D. Ugolini,²³ R. Wang,²³ X. Zhou,²³ T.E. Coan,²⁴ V. Fadeyev,²⁴ I. Korolkov,²⁴ Y. Maravin,²⁴ I. Narsky,²⁴ V. Shelkov,²⁴ J. Staeck,²⁴ R. Stroynowski,²⁴ I. Volobouev,²⁴ J. Ye,²⁴ M. Artuso,²⁵ F. Azfar,²⁵ A. Efimov,²⁵ M. Goldberg,²⁵ D. He,²⁵ S. Kopp,²⁵ G.C. Moneti,²⁵ R. Mountain,²⁵ S. Schuh,²⁵ T. Skwarnicki,²⁵ S. Stone,²⁵ G. Viehhauser,²⁵ and X. Xing²⁵

(CLEO Collaboration)

¹Vanderbilt University, Nashville, Tennessee 37235

²Virginia Polytechnic Institute and State University, Blacksburg, Virginia 24061

³Wayne State University, Detroit, Michigan 48202

⁴California Institute of Technology, Pasadena, California 91125

⁵University of California, San Diego, La Jolla, California 92093

⁶University of California, Santa Barbara, California 93106

⁷University of Colorado, Boulder, Colorado 80309-0390

⁸Cornell University, Ithaca, New York 14853

⁹University of Florida, Gainesville, Florida 32611

¹⁰Harvard University, Cambridge, Massachusetts 02138

¹¹University of Hawaii at Manoa, Honolulu, Hawaii 96822

¹²University of Illinois, Urbana-Champaign, Illinois 61801

¹³Carleton University, Ottawa, Ontario, Canada K1S 5B6

and the Institute of Particle Physics, Canada

¹⁴McGill University, Montréal, Québec, Canada H3A 2T8

and the Institute of Particle Physics, Canada

¹⁵Ithaca College, Ithaca, New York 14850

¹⁶University of Kansas, Lawrence, Kansas 66045

¹⁷University of Minnesota, Minneapolis, Minnesota 55455

¹⁸State University of New York at Albany, Albany, New York 12222

¹⁹Ohio State University, Columbus, Ohio 43210

²⁰University of Oklahoma, Norman, Oklahoma 73019

²¹Purdue University, West Lafayette, Indiana 47907

²²University of Rochester, Rochester, New York 14627

²³Stanford Linear Accelerator Center, Stanford University, Stanford, California 94309

²⁴Southern Methodist University, Dallas, Texas 75275

²⁵Syracuse University, Syracuse, New York 13244

(Received 19 November 1997)

We have observed a signal for the decay $D^{*+} \rightarrow D^+ \gamma$ at a significance of 4 standard deviations. From the measured branching ratio $\mathcal{B}(D^{*+} \rightarrow D^+ \gamma)/\mathcal{B}(D^{*+} \rightarrow D^+ \pi^0) = 0.055 \pm 0.014 \pm 0.010$ we find $\mathcal{B}(D^{*+} \rightarrow D^+ \gamma) = 0.017 \pm 0.004 \pm 0.003$, where the first uncertainty is statistical and the second is systematic. We also report the highest precision determination of the remaining D^{*+} branching fractions. [S0031-9007(98)05932-8]

PACS numbers: 13.20.Fc, 12.39.Fe, 13.40.Hq, 14.40.Lb

The decays of the excited charmed mesons, D^{*+} and D^{*0} , have been the subject of extensive theoretical [1–4] as well as experimental [5–11] investigation. The decay of the D^{*0} via emission of a π^0 or a photon has been observed and its branching ratio well measured [12]. While the D^{*+} hadronic decays ($D^{*+} \rightarrow D^+ \pi^0$ and $D^{*+} \rightarrow D^0 \pi^+$) [13] have been observed and are widely used to tag heavy quark decays, the observation of the D^{*+} radiative decay remained problematic. Both D^* mesons decay electromagnetically as the result of a spin-flip of either the charm quark or the light quark. In the case of the D^{*0} , the decay amplitudes for these two processes interfere constructively. Combined with the phase space suppression of the hadronic decay, this interference results in a radiative decay fraction which competes with the hadronic decay fraction. In the case of the D^{*+} , the amplitudes for the two spin-flip processes interfere destructively. Also, there is slightly more phase space available for the hadronic decay. These two conditions result in a radiative decay fraction of the D^{*+} which, in comparison to the D^{*0} , is significantly suppressed relative to the hadronic decay fraction.

A great deal of interest in the radiative D^{*+} decay was generated by an earlier Particle Data Group (PDG) average of $\mathcal{B}(D^{*+} \rightarrow D^+ \gamma) = (18 \pm 4)\%$ [14]; this value was virtually impossible to reconcile with theory without assuming an anomalously large magnetic moment for the charm quark [4]. Based on 780 pb^{-1} of data, a previous CLEO II analysis [10] found an upper limit of 4.2% (90% C.L.) for this branching fraction, a result which strongly affected not only the D^{*+} branching fractions but also many B measurements. In addition to its importance in measuring B meson decays, a precision determination of the D^{*+} branching fractions will provide an important test of many quark models and other theoretical approaches to heavy meson decays [1]. For theories built around chiral and heavy-quark symmetry (heavy hadron chiral perturbation theory) [2], this measurement will also provide a strong constraint on the two input parameters (g and β) allowing model-independent predictions to be made on a wide variety of observable quantities [3].

The approach used in this analysis is to search in the $\Delta M_\gamma \equiv M(D^+ \gamma) - M(D^+)$ [15] and $\Delta M_\pi \equiv M(D^+ \pi^0) - M(D^+)$ distributions for D^{*+} events using the decay chain $D^{*+} \rightarrow D^+ (\gamma \text{ or } \pi^0)$, $D^+ \rightarrow K^- \pi^+ \pi^+$. The branching ratio

$$R_\gamma^+ \equiv \frac{\mathcal{B}(D^{*+} \rightarrow D^+ \gamma)}{\mathcal{B}(D^{*+} \rightarrow D^+ \pi^0)} = \frac{N(D^+ \gamma)}{N(D^+ \pi^0)} \times \frac{\epsilon_{\pi^0}}{\epsilon_\gamma} \quad (1)$$

is then determined, where $N(D^+ \gamma)/N(D^+ \pi^0)$ is the ratio

of the number of D^{*+} decays observed in each mode, and $\epsilon_{\pi^0}/\epsilon_\gamma$ is the relative efficiency for finding the π^0 or the γ from the corresponding D^{*+} decay. Assuming that the three decay modes of the D^{*+} add to unity and defining $R_\pi^+ \equiv \mathcal{B}(D^{*+} \rightarrow D^0 \pi^+)/\mathcal{B}(D^{*+} \rightarrow D^+ \pi^0)$, one finds $\mathcal{B}(D^{*+} \rightarrow D^+ \gamma) = R_\gamma^+/(R_\gamma^+ + R_\pi^+ + 1)$, $\mathcal{B}(D^{*+} \rightarrow D^+ \pi^0) = 1/(R_\gamma^+ + R_\pi^+ + 1)$, and $\mathcal{B}(D^{*+} \rightarrow D^0 \pi^+) = R_\pi^+/(R_\gamma^+ + R_\pi^+ + 1)$. A value for R_π^+ can be obtained by combining the known phase space for $D^{*+} \rightarrow D^+ \pi^0$ and $D^{*+} \rightarrow D^0 \pi^+$ with isospin conservation and the expected p^3 dependence of p -wave decay widths to yield

$$R_\pi^+ = 2 \left(\frac{p_{+0}}{p_{++}} \right)^3 = 2.199 \pm 0.064, \quad (2)$$

(where p_{+0} and p_{++} are the momenta of the D^0 and D^+ in the D^{*+} rest frame, respectively). The theoretical uncertainty in this ratio is thought to be only of the order of 1% [4], so the error is dominated by those due to the $M_{D^*} - M_D$ mass differences [12]. This method has the advantage of avoiding large systematic uncertainties due to the D meson branching fractions and of canceling many systematic uncertainties associated with the D^+ reconstruction.

The analysis was performed using data accumulated by the CLEO II detector [16] at the Cornell Electron Storage Ring (CESR). The CLEO II detector consists of three cylindrical drift chambers (immersed in a 1.5 T solenoidal magnetic field) surrounded by a time-of-flight system (TOF) and a CsI crystal electromagnetic (EM) calorimeter. The main drift chamber allows for charged particle identification via specific-ionization measurements (dE/dx) in addition to providing an excellent momentum measurement. The calorimeter is surrounded by a superconductor coil and an iron flux return, which is instrumented with muon counters.

A total of 4.7 fb^{-1} of data was collected at center-of-mass energies on or near the $\Upsilon(4S)$ resonance. The Monte Carlo simulated events used to determine signal shapes and detection efficiencies were produced with a GEANT-based full detector simulation.

Events were required to have three or more tracks and at least 15% of the center-of-mass energy deposited in the calorimeter. Each of the three tracks comprising a candidate $D^+ \rightarrow K^- \pi^+ \pi^+$ decay was required to satisfy either the K^- or π^+ hypothesis at the 2.5σ level using dE/dx alone, and then the triplet was required to satisfy the $K^- \pi^+ \pi^+$ hypothesis, including TOF information if available, with a χ^2 probability greater than 10%. The three tracks were then constrained to come from a common vertex, and the invariant mass of the triplet,

under the $K^- \pi^+ \pi^+$ hypothesis, was required to be within 10 MeV/ c^2 ($\sim 1.5\sigma$) of the known D^+ mass.

Photon candidates were required to be in the best region of the calorimeter, $|\cos \theta| < 0.71$ (where θ is the polar angle between the EM cluster centroid and the beam axis), with a cluster energy of at least 30 MeV. It was further required that no charged particle track point within 8 cm of a crystal used in the EM cluster. If the invariant mass formed by a pair of photons was within 2.5σ of the π^0 mass, taking into account the asymmetric π^0 line shape and the small momentum dependence of the mass resolution, the photons were identified as being from a π^0 . The photons were then kinematically constrained to the π^0 mass to improve the π^0 momentum measurement.

Photons from $D^{*+} \rightarrow D^+ \gamma$ decays were required to pass a lateral shower shape cut, which is 99% efficient for isolated photons, and not to form a π^0 when paired with any other photon. For the momenta relevant to D^{*+} decays at the Y(4S), merging of the EM clusters from a π^0 decay (and the subsequent misidentification of a radiative decay) does not occur. The decay angle θ_γ , defined as the angle of the γ in the D^{*+} rest frame with respect to the D^{*+} 's direction in the laboratory frame, was required to satisfy $\cos \theta_\gamma > -0.35$. This cut helps to reduce the large combinatorial background that arises when D^+ mesons are combined with soft photons moving in the opposite direction.

The combinatorial background was further reduced by requiring $x_{D^+} > 0.7$, where x_{D^+} is the fraction of the maximum possible momentum carried by the reconstructed D^{*+} . This cut also removed any contribution from $B \rightarrow D^* X$ events. The cuts on $\cos \theta_\gamma$ and x_{D^+} were determined to maximize S^2/B (S is signal and B is background) by utilizing a large sample of $D^{*0} \rightarrow D^0 \gamma$ events from the data as well as Monte Carlo simulated events.

The primary difficulty in this analysis is the small size of the signal, due to the branching fraction, relative to a large combinatorial background and, more importantly, relative to a background due to D_s^{*+} radiative decays where $D_s^{*+} \rightarrow K^- K^+ \pi^+$. Unlike the D^{*+} , the D_s^{*+} almost always decays radiatively. This is a major problem because the $M(D_s^{*+}) - M(D_s^+)$ mass difference is 143.97 ± 0.41 MeV [17] and the $M(D^{*+}) - M(D^+)$ mass difference is 140.64 ± 0.09 MeV [12], so these two processes cannot be separated in the mass difference plot because the resolution in photon energy in the decay is ~ 6 MeV. Misidentification of $D_s^{*+} \rightarrow K^- K^+ \pi^+$ as $D^+ \rightarrow K^- \pi^+ \pi^+$ can occur because the TOF and dE/dx information used for particle identification does not adequately separate K 's from π 's with momenta above ~ 1 GeV/ c . When reconstructed under the $K\pi\pi$ hypothesis, the two invariant mass distributions partially overlap, and any attempt to estimate the fraction of D_s^{*+} under the D^+ peak will depend strongly on the resonant substructure of the $D_s^{*+} \rightarrow K^- K^+ \pi^+$ decay, as well as the momentum distribution of the D_s^{*+} 's. The large D_s^{*+} contribution to the lower D^+ sideband further complicates the analysis

by preventing the use of this sideband in a subtraction of combinatorial background. Because of its small rate ($< 0.2\%$ of the signal), no correction is necessary to address the presence of the recently observed hadronic decay $D_s^{*+} \rightarrow D_s^+ \pi^0$ [17] in the ΔM_π distribution.

A means to veto D_s^{*+} events, independent of the decay's resonant substructure, is to require that the invariant mass of the three tracks reconstructed under the $K^- K^+ \pi^+$ hypothesis be greater than a cut which removes all the D_s^{*+} events. An unwanted side effect of vetoing D_s^{*+} events by this method is that a cut in the $KK\pi$ mass distribution greatly distorts the $K\pi\pi$ mass distribution, making the relative normalization between the D^+ upper sideband and the signal region uncertain. Thus, the use of a sideband subtraction to remove the combinatorial background from the mass difference plot is impossible. Figure 1 shows the Monte Carlo $K^- K^+ \pi^+$ mass distribution found in D_s^{*+} decays and that found in D^+ decays when one of the π^+ 's is misidentified as a K^+ . Since there are two possible tracks to assign the K^+ mass, both combinations are tried, and the one yielding the smaller mass is plotted.

Figure 2(a) shows the ΔM_γ distribution for events from the $M(D^+)$ signal region as well as for those from the $M(D^+)$ upper sideband (a region 3 times as wide as the signal region starting $\approx 3\sigma$ above the nominal D^+ mass). The ΔM_γ distribution for the combinatorial background found in the $M(D^+)$ sideband is quite flat under the signal region, justifying the use of a first order polynomial in fitting this background. No D_s^{*+} veto has been applied to the data in Fig. 2(a), so a fair fraction of the events in this "signal" are D_s^{*+} background. The signal was fit with a modified Gaussian, the parameters for which were obtained from a large Monte Carlo sample of $D^{*+} \rightarrow D^+ \gamma$ events. The systematic error in the fit parameters was estimated by studying data versus Monte Carlo differences in the very similar decay $D^{*0} \rightarrow D^0 \gamma$.

Figure 2(b) shows the ΔM_γ signal and sideband distributions for events satisfying the D_s^{*+} veto requirement that $M(K^- K^+ \pi^+) > 1.990$ GeV/ c^2 . Monte Carlo indicates the fraction of D_s^{*+} events passing this cut is $0.002^{+0.003}_{-0.002}$, thus if the entire signal yield (180 ± 26 events) found in Fig. 2(a) were due to D_s^{*+} decays, $0.4^{+0.6}_{-0.4}$ events would be expected in Fig. 2(b). The fit to

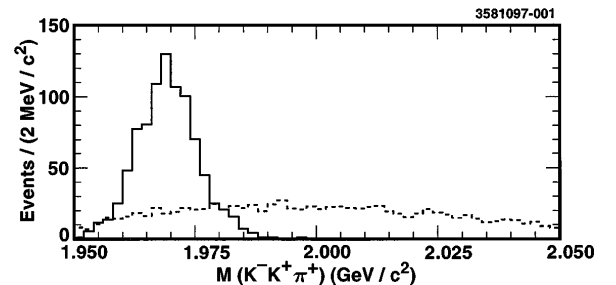


FIG. 1. The $M(K^- K^+ \pi^+)$ distributions for D_s^{*+} background (solid line) and D^+ signal (dashed line) Monte Carlo samples.

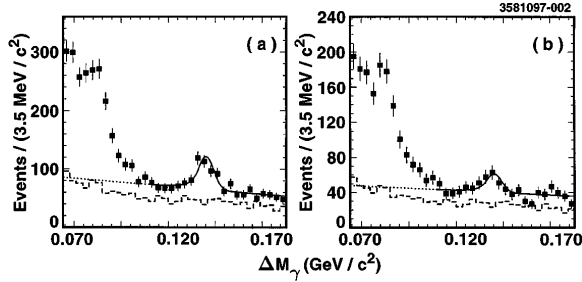


FIG. 2. The $\Delta M_\gamma \equiv M(D^+\gamma) - M(D^+)$ distributions for (a) data before the D_s^{*+} veto has been applied, (b) data after the tight D_s^{*+} veto has been applied. The large feature on the left of the plots is due to $D^{*+} \rightarrow D^+\pi^0$, where one of the photons from the π^0 decay is not detected. Monte Carlo studies indicate that this decay does not contribute to the signal region. The dashed histograms are data taken from the upper $M(D^+)$ sideband.

the ΔM_γ distribution in Fig. 2(b) yields 68 ± 19 events. When these data are refit with the signal constrained to be $0.4^{+0.6}_{-0.4}$ events, the χ^2 of the fit increases by 15.8, corresponding to a significance of 4.0 standard deviations that the signal is not due to misidentified D_s^{*+} events. Therefore, the peak must be due to the decay $D^{*+} \rightarrow D^+\gamma$.

The presence of $D^{*+} \rightarrow D^+\gamma$ decays having been established, the D_s^{*+} veto was loosened to $1.981 \text{ GeV}/c^2$ to maximize $S^2/(S+B)$ as determined by the Monte Carlo samples. Figure 3(a) shows the ΔM_γ distribution for the events which passed the optimized D_s^{*+} veto. The fraction of D^+ mesons passing the veto was determined by fitting the ΔM_π distribution before and after the veto was applied to the data. These distributions were fit with

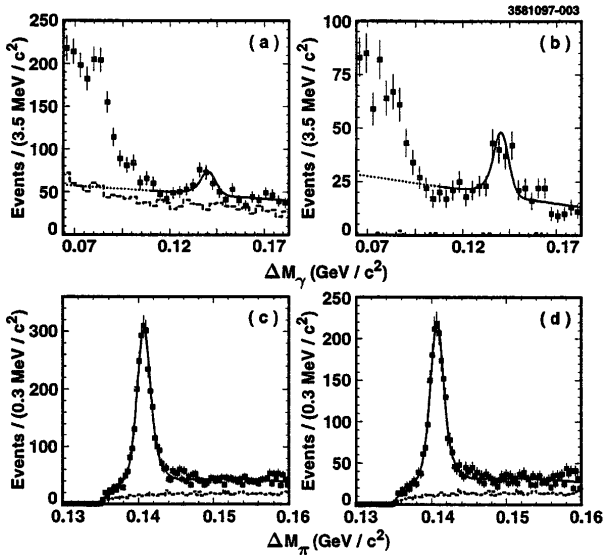


FIG. 3. (a) ΔM_γ distribution for data after the “optimal” $M(K^-K^+\pi^+)$ cut (the D_s^{*+} veto) has been applied. (b) ΔM_γ distribution for the vetoed data. (c) ΔM_π distribution for data prior to the $M(K^-K^+\pi^+)$ cut. (d) ΔM_π distribution for data after the $M(K^-K^+\pi^+)$ cut is applied. The dashed histograms are data taken from the upper $M(D^+)$ sideband.

a double Gaussian plus a background function [18] which simulates the expected threshold behavior. Figures 3(c) and 3(d) show the ΔM_π distributions, along with the fits, used to determine the D_s^{*+} veto efficiency for D^+ mesons.

The results of fitting the ΔM_γ distribution for events which passed and for those which failed the D_s^{*+} veto, Figs. 3(a) and 3(b), respectively, were: $N_\gamma^{\text{pass}} = 87 \pm 21$ and $N_\gamma^{\text{fail}} = 95 \pm 16$ (statistical errors only). Defining N_+ (N_s) as the total number of D^{*+} (D_s^{*+}) in the data, one has the following pair of equations:

$$\begin{aligned} (1 - \epsilon_+)N_+ + (1 - \epsilon_s)N_s &= N_\gamma^{\text{fail}}, \\ \epsilon_+N_+ + \epsilon_sN_s &= N_\gamma^{\text{pass}}, \end{aligned} \quad (3)$$

where ϵ_+ is the fraction of D^{*+} 's which pass the veto as determined by fitting the ΔM_π distributions ($N_\pi^{\text{pass}} = 1650 \pm 57$ and $N_\pi^{\text{total}} = 2265 \pm 66$, where the errors are statistical only), and $\epsilon_s = 0.037 \pm 0.007$ is the fraction of D_s^{*+} 's which escape the veto as determined by a Monte Carlo study. Rewriting Eq. (3) in terms of the measured quantities (N_γ^{pass} , N_γ^{fail} , N_π^{pass} , N_π^{total}) and ϵ_s and solving for R_γ^+ , we find

$$\begin{aligned} R_\gamma^+ &= \frac{N_\gamma^{\text{pass}} - \epsilon_s(N_\gamma^{\text{fail}} + N_\gamma^{\text{pass}})}{N_\pi^{\text{pass}} - \epsilon_s N_\pi^{\text{total}}} \times \frac{\epsilon_{\pi^0}}{\epsilon_\gamma} \\ &= 0.055 \pm 0.014 \pm 0.010, \end{aligned} \quad (4)$$

where the ratio of efficiencies $\epsilon_{\pi^0}/\epsilon_\gamma = 1.066 \pm 0.064$. From this branching ratio we can then extract the branching fractions shown in Table I. The statistical uncertainty is dominated by the $D^+\gamma$ yields, and the largest systematic uncertainty is due to variations in this yield, when the mean and width of the signal shape were varied by an amount suggested by the $D^{*0} \rightarrow D^0\gamma$ data versus Monte Carlo comparison. A similar comparison was used to estimate the uncertainty introduced by the $\cos\theta_\gamma$ cut. Table II lists the various sources of systematic uncertainty and gives estimates for their impact on the measurement of R_γ^+ .

In conclusion, we have observed, with 4σ significance, the radiative decay of the D^{*+} and measured $\mathcal{B}(D^{*+} \rightarrow D^+\gamma)/\mathcal{B}(D^{*+} \rightarrow D^+\pi^0) = 0.055 \pm 0.017$ (statistical and systematic uncertainties added in quadrature). Assuming Eq. (2) and that the three branching fractions of the D^{*+} add to unity, we find the results in Table I. The hadronic branching fractions are in good agreement with

TABLE I. The $D^*(2010)^\pm$ branching fractions determined from the measured ratio $N(D^+\gamma)/N(D^+\pi^0)$. The first uncertainty is statistical, the second is experimental systematic and the third is that which arises from the use of Eq. (2).

Mode	CLEO II	PDG [12]
$D^+\gamma$	$(1.68 \pm 0.42 \pm 0.29 \pm 0.03)\%$	$(1.1^{+2.1}_{-0.7})\%$
$D^+\pi^0$	$(30.73 \pm 0.13 \pm 0.09 \pm 0.61)\%$	$(30.6 \pm 2.5)\%$
$D^0\pi^+$	$(67.59 \pm 0.29 \pm 0.20 \pm 0.61)\%$	$(68.3 \pm 1.4)\%$

TABLE II. Estimates of the systematic uncertainties in the measurement of R_γ^+ .

Efficiency ratio $\epsilon_{\pi^0}/\epsilon_\gamma$	6%
Fitting of background	9%
Fitting of signal	13%
Veto efficiency for D_s^+ (19% on ϵ_s)	1%
Veto efficiency for D^+ (2% on ϵ_+)	2%
$\cos \theta_\gamma > -0.35$	5%

the current PDG averages [12], but with substantially reduced uncertainties (which are now dominated by the 3% uncertainty in R_π^+). The D^{*+} radiative branching fraction is in good agreement with theoretical expectations and the earlier upper limits set by CLEO II [10] and ARGUS [11]. The uncertainty in this branching fraction is due primarily to the large combinatorial background under the radiative signal, so one can expect that data taken with the new CLEO II.5 detector, which includes a silicon tracker, will reduce this uncertainty further in the near future.

We gratefully acknowledge the effort of the CESR staff in providing us with excellent luminosity and running conditions. This work was supported by the National Science Foundation, the U.S. Department of Energy, the Heisenberg Foundation, the Alexander von Humboldt Stiftung, Research Corporation, the Natural Sciences and Engineering Research Council of Canada, the A. P. Sloan Foundation, and the Swiss National Science Foundation.

*Permanent address: Brookhaven National Laboratory, Upton, NY 11973.

†Permanent address: University of Texas, Austin, TX 78712.

‡Permanent address: Lawrence Livermore National Laboratory, Livermore, CA 94551.

§Permanent address: BINP, RU-630090 Novosibirsk, Russia.

||Permanent address: Yonsei University, Seoul 120-749, Korea.

- [1] See, for example, A.N. Kamal and Q.P. Xu, Phys. Lett. B **284**, 421 (1992); P.J. O'Donnell and Q.P. Xu, Phys. Lett. B **336**, 113 (1994); P. Colangelo, F. De Fazio, and

G. Nardulli, Phys. Lett. B **334**, 175 (1994); T.M. Aliev *et al.*, Phys. Rev. D **54**, 857 (1996); H.G. Dosch and S. Narison, Phys. Lett. B **368**, 163 (1996).

- [2] M.B. Wise, Phys. Rev. D **45**, R2188 (1992); G. Burdman and J. Donoghue, Phys. Lett. B **280**, 287 (1992); H.Y. Cheng *et al.*, Phys. Rev. D **49**, 5857 (1994); *ibid.* **55**, 5851(E) (1997); R. Casalbuoni *et al.*, Phys. Rep. **281**, 145 (1997).
- [3] J. Admundson *et al.*, Phys. Lett. B **296**, 415 (1992); P. Cho and H. Georgi, Phys. Lett. B **296**, 408 (1992); *ibid.* **300**, 410(E) (1993).
- [4] E. Angelos and G.P. Lepage, Phys. Rev. D **45**, R3021 (1992).
- [5] Mark I Collaboration, G. Goldhaber *et al.*, Phys. Lett. **69B**, 503 (1977).
- [6] Mark II Collaboration, M.W. Coles *et al.*, Phys. Rev. D **26**, 2190 (1982).
- [7] JADE Collaboration, W. Bartelt *et al.*, Phys. Lett. **161B**, 197 (1985).
- [8] HRS Collaboration, E.H. Low *et al.*, Phys. Lett. B **183**, 232 (1987).
- [9] Mark III Collaboration, J. Adler *et al.*, Phys. Lett. B **208**, 152 (1988).
- [10] CLEO Collaboration, F. Butler *et al.*, Phys. Rev. Lett. **69**, 2041 (1992).
- [11] ARGUS Collaboration, H. Albrecht *et al.*, Z. Phys. C **66**, 63 (1995).
- [12] Particle Data Group, R.M. Barnett *et al.*, Phys. Rev. D **54**, 1 (1996).
- [13] Inclusion of the charge conjugate reaction is implied throughout this paper.
- [14] Particle Data Group, J.J. Hernández *et al.*, Phys. Lett. B **239**, 1 (1990).
- [15] $M(X)$ refers to the invariant mass of the particles used to form the X candidate.
- [16] CLEO Collaboration, Y. Kubota *et al.*, Nucl. Instrum. Methods Phys. Res., Sect. A **320**, 66 (1992).
- [17] CLEO Collaboration, J. Gronberg *et al.*, Phys. Rev. Lett. **75**, 3232 (1995).
- [18] The total area as well as the mean and sigma of the primary Gaussian (62% of the signal) were allowed to float while the ratio of the areas, means, and sigmas were fixed to the values obtained from the Monte Carlo sample. The background function used is $p_1[(\Delta M_\pi - M_{\pi^0})^{1/2} + p_2(\Delta M_\pi - M_{\pi^0})^{3/2}]$, where p_1 and p_2 are parameters determined by the fit.